

DELFT UNIVERSITY OF TECHNOLOGY

BACHELOR THESIS

TU DELFT, BSc APPLIED PHYSICS AND BSc APPLIED
MATHEMATICS

Modelling Polyelectrolyte Multilayer Growth

Author:
Dennis BOUWMAN

Supervisors:
Dr. Ir. D. DEN OUDEN
Dr. Ir. N.A.M. BESSELING

September 29, 2016



Contents

1	Introduction	1
2	A Model for Polyelectrolyte Multilayers	3
2.1	Layer-by-Layer Assembly	3
2.2	Diffusion Equations	4
2.3	Boundary Conditions	5
2.4	Equilibrium Conditions	7
2.4.1	Phase Equilibrium	7
2.4.2	Equilibrium Conditions on the Interface	9
2.5	Analytical Reduction of the Model	9
3	Numerical Approach	11
3.1	Weak Formulation and Galerkin's Method	11
3.2	The Finite Element Method in \mathbb{R}	12
3.2.1	Assembly of the large matrix and vector	14
3.3	Moving Mesh Method	15
3.4	Galerkin Equations of the Moving-Mesh Diffusion Equation	17
3.4.1	Galerkin Equations in Matrix Form	18
3.4.2	Boundary conditions	20
3.5	Time Step	21
3.6	Fixed Point Iterations	21
3.7	Broyden Iterations	22
3.7.1	Newton's Method and modifications	22
3.7.2	Implementation of Broyden's Method	23
3.7.3	Assuring Convergence of Broydens Method	23
4	Implementation	25
4.1	Initial Condition	25

4.2	Overview of the script	25
4.3	Difficulties & Discussion	27
4.3.1	α -Safety-Protocol	27
4.3.2	Non-convergence	27
4.3.3	Instant Equilibrium Assumption for Small-Ions	28
5	Results	29
5.1	Inconsistency in the Tie Lines	29
5.2	Simulations	31
5.2.1	Profiles near the Substrate	31
5.2.2	Non-Responsive Interface	31
6	Conclusions and Discussion	34
A	Derivation of the Stefan Condition	36
B	Assembly of the Large Discretisation Matrix	39
C	Derivation of the Mesh-Velocity Constraint	41
D	Example of Inconsistent Tie-Line Model	43

Chapter 1

Introduction

In many fields of engineering we can find examples of different uses of thin films. One of these is the organic thin film: polyelectrolyte multilayer (PEM). PEMs can be fabricated with a processes called the Layer by Layer (LbL) assembly. This method was invented by [G. Decher and Schmitt 1992] and proved to be a versatile way of constructing thin layers of polyelectrolytes. Since this publication the LbL assembly method has been a popular field of study. Recently [Tang and Besseling 2015] presented a model in which the formation of PEMs is treated as a phase separation of the polyelectrolytes into a concentrated phase (i.e. thin film) and a dilute phase (i.e. solution). In this study we build on this interpretation, treating the PEM as a concentrated domain with in-state diffusion and a moving interface on which we will apply a model of phase separation to specify boundary conditions. We will restrict our study to a one-dimensional convection-free approach. This model is formally known as a *Stefan Problem*. Furthermore, we will present a numerical approach to find an approximate solution to the set of partial differential equations describing the formation of PEMs.

In the present paper we will model the PEM formation and discuss a phase separation model for finding boundary conditions on the interface. Moreover we will discuss the constraints on the phase separation that were found after scrutinous analysis. Also we will develop the numerical approach to solve the set of non-linear coupled partial differential equations, based upon the Finite-Element Method. Furthermore we will discuss some computational difficulties of this problem and we will present several recommendations for future studies based on the numerical analysis.

During the simulations we concluded that our current model for is not able to ac-

curately describe the behaviour of polyelectrolytes during the formation of PEMs. The main difficulty took place at the interface, which led us to believe that a more in-depth study is needed to find a suitable model for phase separation. However we believe that the numerical approach and the physical interpretation of coexisting phases are promising developments and that future research may lead to accurate simulations for the evolution of PEMs.

This research is performed as a part of the course *Bachelorproject TWN*, to obtain the degrees of *Bachelor of Applied Physics* and *Bachelor of Applied Mathematics* at the Delft University of Technology.

Chapter 2

A Model for Polyelectrolyte Multilayers

2.1 Layer-by-Layer Assembly

The Layer by Layer (LbL) assembly is a way to fabricate polyelectrolyte multilayers (PEM) by dipping a substrate alternatively in solutions of poly-cations and poly-anions. These polyelectrolytes form a layer on the substrate. The formation of this layer is influenced by electrostatic interactions between chemical components. These electrostatic interactions can be influenced by adding a simple salt, e.g. $NaCl$, to the solution. Once in solution, the salt will dissolve into Na^+ and Cl^- , which will be named *small ions* hereafter. We introduce the following notation: $[+] = Z_{P+}c_{P+}$ and $[-] = Z_{P-}c_{P-}$. These are the concentrations of poly-cations and poly-anions respectively, expressed in terms of equivalent charge, where Z_i is the number of elementary charges per molecule. c_{P+} and c_{P-} are the concentration of poly-cations and poly-anions respectively. Typical magnitudes for Z_{P+} and Z_{P-} for polyelectrolytes are between 100 and 100.000. Note that these values of Z are much higher for poly-electrolytes than for small ions, as $Z_{Na^+} = -Z_{Cl^-} = 1$.

During fabrication of a PEM, we can make a distinction between two separate phases. The *concentrated phase* $\Omega_C(t)$ and the *dilute phase* $\Omega_D(t)$. In the concentrated phase, the poly-electrolytes are entangled with one another and make up the film on the substrate. In the dilute phase, a poly-electrolyte is not entangled and is considered to be dissolved. In both phases concentrations of small ions are present. The

position of the interface between the two is defined as $\Gamma(t)$. The distribution of chemical components can be described with the diffusion equation for charged chemical components.

2.2 Diffusion Equations

The diffusion of charged chemical components can be described with a Poisson-Nernst-Planck system of equations. The Nernst-Planck equation is an extension of Fick's Diffusion Law including the influence of an electric field. We can write such a transport equation for each component i :

$$\frac{\partial c_i(z, t)}{\partial t} = -\frac{\partial J_i(z, t)}{\partial z}, \quad (2.1)$$

where the flux $J_i(z, t)$, assuming that convection is negligible, is given by:

$$J_i(z, t) = -D_i \left(\frac{\partial c_i(z, t)}{\partial z} + \frac{Z_i F c_i(z, t)}{RT} \frac{\partial \psi(z, t)}{\partial z} \right). \quad (2.2)$$

In these equations F is Faraday's constant, with its physical meaning of the charge of one mole of elementary charges. $\psi(z)$ is the mean electric potential and D_i is the diffusion coefficient. Note that the flux in Equation (2.2) consists of two distinct terms. The first term accounts for standard diffusion. The second term accounts for drift due to an electric field. If this potential is constant then Equation (2.1) reduces to Fick's Law for diffusion.

In our case the electric potential is the result of the charge distribution of all the chemical components. The relation between the electric potential and the charge distribution is given by the Poisson equation:

$$\frac{\partial^2 \psi(z, t)}{\partial z^2} = -\frac{F}{\epsilon_0 \epsilon_r} \sum_i Z_i c_i(z, t), \quad (2.3)$$

where ϵ_0 and ϵ_r are the vacuum- and relative permittivity respectively.

Finally we shall introduce some reasonable simplifications on the model. First, we assume that the diffusion coefficients are constant, but different, in each phase. So, $D_i = D_i^C$ in the concentrated phase and $D_i = D_i^D$ in the dilute phase. It is important to note that in general $D_i^C \ll D_i^D$, this is due to the structure of the concentrated

phase. As discussed, the polyelectrolytes are entangled and this greatly constraints the movement of polyelectrolytes. This effect also applies to small ions to some extent. The concentration profiles do not have to be continuous across the interface. This also means that the electric potential does not have to be continuous across the interface. This poses some difficulty for finding boundary conditions on the interface.

2.3 Boundary Conditions

Thus far we have developed a model with two distinct domains: $\Omega_C(t)$ and $\Omega_D(t)$. In each of which 4 chemical components are dissolved: $[+]$, $[-]$, $[Na^+]$ and $[Cl^-]$. Each of these components is subjected to a diffusion equation in each domain: Equation (2.1). Also, we have to find an electric potential across the domains which should satisfy Equation (2.3) in each domain. In the present approach Equation (2.3) is not applied to the phase boundary.

If we want to gain insight in how the interface $\Gamma(t)$ evolves in time, then we need to determine the movement of the interface in the normal direction, v_n . Also, we need to know about the equilibrium of coexisting phases, but this subject will be discussed later. If we want to solve this system of equations, then we have to find a sufficient number of boundary and interface conditions.

Lets start with some simple boundary conditions, at $z = 0$ there exist a no-flux boundary condition for the components. This means that the substrate is impenetrable. This gives:

$$J_i(z, t)|_{z=0} = 0. \quad (2.4)$$

On the other side, at $z = z_{max}$ the concentrations of the components are held constant, the value of this constant depends on the experimental setup. This boundary condition simulates the inflow of chemical components. This gives:

$$c_i(z, t)|_{z=z_{max}} = constant. \quad (2.5)$$

Now we shall concern us with the boundary conditions on the interface. These conditions impose an extra difficulty because the phase interface in general has no fixed position, whereas the conditions on $z = 0$ and $z = z_{max}$ are fixed. Therefore we make the following assumption: the transfer of poly-ions between the two phases is not restricted by a reaction constant. In other words, a poly-electrolyte at the interface that wants to enter the other phase can do so instantaneously, this is opposed to

an interface where absorption is dominated by a reaction process. Therefore the concentrations assume equilibrium values on either side of the interface instantaneously. We define $z = z^{IC}$ as the concentrated side of the interface and $z = z^{ID}$ as the dilute side. Then we have the boundary conditions:

$$c_i(z, t) \Big|_{z=z^{IC}} = c_{i,eq}^{IC}(t), \quad (2.6)$$

and

$$c_i(z, t) \Big|_{z=z^{ID}} = c_{i,eq}^{ID}(t). \quad (2.7)$$

Where $c_{i,eq}^{IC}(t)$ and $c_{i,eq}^{ID}(t)$ are the respective equilibrium concentrations at the interface.

Now we will take a look at the velocity of the interface. If an interface is moving then it is subject to the Stefan boundary condition. This boundary condition originates from conservation of mass and therefore has to hold for each chemical component.

$$c_{i,eq}^{IC}(t)v_n(t) - J_i^{IC}(t) = c_{i,eq}^{ID}(t)v_n(t) - J_i^{ID}(t). \quad (2.8)$$

The flux does not have to be continuous across the interface and therefore the subscripts 'IC' and 'ID' are necessary to indicate the concentrated side or the dilute side of the interface. Note that the normal velocity of the interface v_n is defined to be directed *outward* of $\Omega_C(t)$ and *inward* of $\Omega_D(t)$. The derivation and interpretation of Equation (2.8) can be found in Appendix A.

We conclude this section with the boundary conditions on the electric potential. It should come as no surprise that we have two Dirichlet conditions at $z = 0$ and $z = z_{max}$:

$$\psi(0, t) = \psi_0, \quad (2.9)$$

where ψ_0 is due to some characteristic charge of the substrate and

$$\psi(z_{max}, t) = 0. \quad (2.10)$$

Furthermore we define two more Dirichlet boundary conditions to account for the potential step across the interface:

$$\psi(z, t) \Big|_{z=z^{IC}} = \psi^{IC}(t), \quad (2.11)$$

and

$$\psi(z, t) \Big|_{z=z^{ID}} = \psi^{ID}(t). \quad (2.12)$$

2.4 Equilibrium Conditions

2.4.1 Phase Equilibrium

In this section we will look at the equilibrium conditions of phases. We will regard the combination of the two phases as an unstable mixture. With an unstable mixture we mean a mixture that tends to separate into distinct phases. In our model, the solution of poly-electrolytes and small ions is obviously not stable. We rather say, the solution is in the phase-coexistence of $\Omega_C(t)$ with $\Omega_D(t)$. To describe the proportions of these phases in equilibrium we make use of a phase diagram. In a phase diagram we set the poly-cation charge concentration on the vertical axis and the poly-anion charge concentration on the horizontal axis. Every point in this diagram corresponds to some initial mixture of respective concentrations. In this diagram we draw two important types of curves. First is the binodal curve: this curve, graphed as an ellipse in the phase diagram, determines the unstable (inside of the ellipse) and stable (outside of the ellipse) regions in the phase diagram. If some initial mixture is in the unstable region of the binodal curve then it is considered unstable and will tend to separate into two distinct stable coexisting phases. The second type of curves are the tie lines. A tie line connects two points on the binodal that represent coexisting phases. In other words, the compositions of the stable coexisting phases in which an initial mixture will separate can be found by looking at the intersections of the binodal curve and the tie lines. An example of such a phase diagram can be found in [Tang and Besseling 2015]. With this important property in mind we will take a closer look at the binodal curve and tie lines.

We simplify our model with very simple binodal curves and tie lines. Our binodal curves are given by:

$$[-]^D = C^D + [+]^D \text{ for the dilute phase and} \quad (2.13)$$

$$[-]^C = C^C + [+]^C \text{ for the concentrated phase.} \quad (2.14)$$

The parameters $C^C, C^D < 0$ are considered to be known. For physical reasons it must hold that $C^C < C^D$. It can easily be verified by noting that $C^C = C^D$ implies that there is no phase separation and $C^C > C^D$ implies that the coexisting dilute phase is more concentrated than the concentrated phase, which would be infeasible. For the tie lines we use the equation:

$$[-] = \kappa[+], \quad (2.15)$$

with $-\infty \leq \kappa < 0$.

Note that there must be a tie line for every unstable mixture. Therefore the parameter κ specifies a particular tie line but also it gives information about the coexisting phases in equilibrium. To make this point more clear, we rewrite equations (2.13) through (2.15) into:

$$\left\{ \begin{array}{l} [-]^D = \frac{\kappa}{\kappa-1} C^D \\ [+]^D = \frac{1}{\kappa-1} C^D \\ [-]^C = \frac{\kappa}{\kappa-1} C^C \\ [+]^C = \frac{1}{\kappa-1} C^C \end{array} \right. \quad (2.16)$$

It can be seen that, for given C^C and C^D , the unknown parameter κ completely determines the coexisting phases. The phase diagram can be seen in Figure 2.1. One can observe that for κ close to -1 , this is a very reasonable assumption.

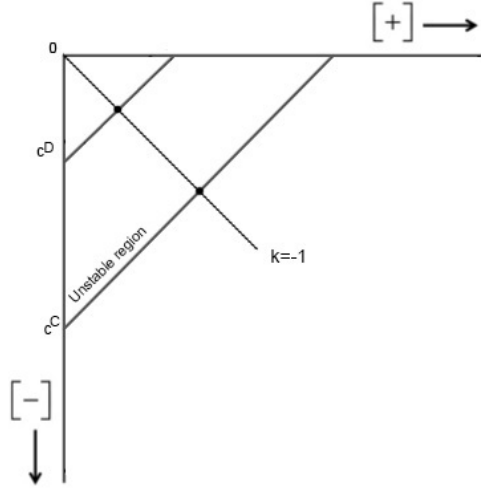


Figure 2.1: The phase diagram with simplified binodal curves and tie lines. For example $\kappa = -1$ is drawn.

Furthermore, the phases should be neutral with respect to charges. It would be the same to state that:

$$[+]^C + [Na^+]^C = -([-]^C + [Cl^-]^C), \quad (2.17)$$

$$[+]^D + [Na^+]^D = -([-]^D + [Cl^-]^D). \quad (2.18)$$

2.4.2 Equilibrium Conditions on the Interface

In our model, the small ions and the electric potential will behave according to a Donnan-type equilibrium. A Donnan-type equilibrium is a situation where a semi-permeable membrane obstructs large molecules (the poly-electrolytes in our case) to diffuse in a coexisting phase setup. However, small ions can penetrate this membrane and therefore there will not be an ‘ordinary’ equilibrium. In a two-phase model, it is known that the phases are in equilibrium if their respective chemical potentials μ are equal:

$$\mu^C = \mu^D, \text{ where } \mu^i = \mu^* + RT \log \left(\frac{[Na^+]^i [Cl^-]^i \gamma_{NaCl,i}}{(c_i^*)^2} \right), \quad (2.19)$$

in this equation there are a few aspects that deserve some attention. μ^* is a material property, and thus the same for both phases. $(c_i^*)^2$ is a constant to make the argument of the logarithm dimensionless and is also the same for both phases. The activity coefficient $\gamma_{NaCl,i} = 1$, that is to say that we consider the simple salt solution as ideal-dilute. If we consider these aspects, then at equilibrium it must hold that:

$$[Na^+]^C [Cl^-]^C = [Na^+]^D [Cl^-]^D. \quad (2.20)$$

Because we assumed in Equations (2.6) and (2.7) that on the interface the concentrations are at equilibrium therefore Equation (2.20) must hold on $\Gamma(t)$. There are also some difficulties with the calculation of the potential across the interface. Because the concentration profiles are not continuous we cannot, in general, find the electric potential step on the interface with the Poisson equation, Equation (2.3). However, we can find this step with the Nernst Equation, which relates it to the equilibrium concentrations of the simple salt on either sides:

$$\psi^{IC} - \psi^{ID} = -\frac{k_B T}{q} \log \left(\frac{[Na^+]^{IC}}{[Na^+]^{ID}} \right) = +\frac{k_B T}{q} \log \left(\frac{[Cl^-]^{ID}}{[Cl^-]^{IC}} \right). \quad (2.21)$$

These conditions are sufficient to solve the problems with the electric potential which arise if the interface is considered as a discontinuity.

2.5 Analytical Reduction of the Model

The model presented in the previous sections allows for some analytical simplification. By combining equations, in a similar fashion as performed to obtain Equation

(2.16), we shall perform a reduction of the model. We start with the equations for electric neutrality and their effect on the phase equilibrium conditions. Specifically the substitution of Equation (2.16) and Equations (2.17) and (2.18). From this we find:

$$[Na^+]^{IC} = -[Cl^-]^{IC} - C^C \left(\frac{\kappa + 1}{\kappa - 1} \right), \quad (2.22)$$

$$[Na^+]^{ID} = -[Cl^-]^{ID} - C^D \left(\frac{\kappa + 1}{\kappa - 1} \right). \quad (2.23)$$

Now we take a closer look at the interface conditions at equilibrium. We will substitute the expressions we found from the previous result into Equation (2.20). We shall then derive an expression for κ :

$$\begin{aligned} [Na^+]^C [Cl^-]^C &= [Na^+]^D [Cl^-]^D, \\ \left(-[Cl^-]^C - C^C \left(\frac{k+1}{k-1} \right) \right) [Cl^-]^C &= \left(-[Cl^-]^D - C^D \left(\frac{k+1}{k-1} \right) \right) [Cl^-]^D, \\ \left(\frac{k+1}{k-1} \right) &= \frac{([Cl^-]^C)^2 - ([Cl^-]^D)^2}{C^D [Cl^-]^D - C^C [Cl^-]^C} (= \tau), \\ k &= \frac{\tau + 1}{\tau - 1}. \end{aligned}$$

Furthermore, given ψ^{ID} we can find an expression for the potential step Equation (2.21):

$$\psi^{IC} = \psi^{ID} - \frac{k_B T}{q} \log \left(\frac{[Cl^-]^{IC}}{[Cl^-]^{ID}} \right) \quad (2.24)$$

To conclude: if the parameters $[Cl^-]^{IC}$, $[Cl^-]^{ID}$, ψ^{ID} , v_n are known then we can calculate the remaining parameters: κ , $[+]^{IC}$, $[-]^{IC}$, $[+]^{ID}$, $[-]^{ID}$, $[Na^+]^{ID}$, $[Na^+]^{IC}$, ψ^{IC} with the above defined equations. However, these 4 parameters are not known. In Section 3.7 we will discuss how we can find an approximation of these parameters. This will finish the physical side of the model. If all the parameters are known then we have properly defined all the boundary conditions. After this the mathematics shall provide us with an approximation for the concentration profiles after a small time step and we can start the whole process of finding the proper boundary conditions again.

Chapter 3

Numerical Approach

This chapter contains all the necessary mathematics that was used during the project. We start with some general theory about the weak formulation of a partial differential equation. Secondly, we present a one dimensional Finite Element Method. We continue by discussing how to track the interface with a moving mesh. Then we combine all the theory to define the Galerkin Equations in matrix form of this problem, also we will show how to apply boundary conditions. Furthermore we explain how we found the solution of the Galerkin Equations, which are defined implicitly. We end this chapter with a section on Broyden Iterations, this numerical method is necessary to approximate the interface conditions.

3.1 Weak Formulation and Galerkin's Method

Every PDE can be expressed in an alternative but equivalent form called the weak formulation. The solution of this weak formulation therefore is equivalent to the solution of the PDE. Therefore instead of solving our PDE directly, we find our solution by defining and solving the weak form.

The reason we want to express a PDE in this alternative form is that this weak form can be solved by the Finite Elements Method (FEM), a powerful numerical technique which is used extensively in this research. More information about FEM can be found in the following section. For now, we will concern us with a general PDE on a domain Ω of the form:

$$Lu = f, \tag{3.1}$$

where $u \in \Sigma$ and $\Sigma = \{u : u \text{ is smooth}\}$. Further L is the differential operator defined over a space Ω and f is a function independent of u . Let us subtract f from the right-hand side, multiply by some arbitrary test function $v \in \Sigma_0$. Where $\Sigma_0 = \{v : v \text{ is smooth, } v = 0 \text{ when } u = u_0\}$, thus if u has an inhomogeneous Dirichlet boundary condition, then we choose v to be zero on that boundary. Then integrate over the domain Ω to obtain:

$$\int_{\Omega} (vLu - vf) d\Omega = 0, \quad \text{for every } v. \quad (3.2)$$

In general L can contain any higher order derivatives. If that is the case, it is necessary to use Gauss' Theorem to reduce the higher order derivatives to the lowest order possible. Equation (3.2) reduced to the lowest possible order of derivatives is called the weak form of Equation (3.1).

To find the solution of the weak form we shall use Galerkin's Method. This method is based on the approximation of the unknown solution u by a finite linear combination of basis functions:

$$u^k(\bar{z}) = \sum_{q=1}^k u_q \phi_q(\bar{z}), \quad (3.3)$$

and substitute this in the weak form, Equation (3.2). After substitution we are left with k unknowns corresponding with the coefficients of the approximation of u . So for a unique solution we need k equations. These can be obtained by choosing the arbitrary test function to be one of the basis functions ϕ_p . After these substitutions we are left with k equations with k unknowns:

$$\sum_{q=1}^k u_q \int_{\Omega} \phi_p L \phi_q d\Omega = \int_{\Omega} \phi_p f d\Omega, \quad \text{for every } p = 1 \dots k. \quad (3.4)$$

These equations are called the Galerkin Equations and they provide the means to approximate the solution of the PDE by obtaining the unknown coefficients u_q who together with the chosen basis functions construct $u^k(\bar{z})$, the solution of the weak form.

3.2 The Finite Element Method in \mathbb{R}

The previous section provided us with a set of equations called the Galerkin Equations which provide the means to approximate the solution of the weak form of a

PDE and equivalently the solution of the PDE itself. In this approach a set of arbitrary basis functions $\{\phi_q\}_{q=1}^k$ plays an important role. The Finite-Elements Method is concerned with choosing this set of basis functions. The main idea behind FEM is to divide the domain Ω into subparts called “elements”. Each basis function then can be defined on each element separately and we can perform element-wise approximations. Moreover, with this method we can formulate the Galerkin Equations as a matrix-vector product. This discretisation makes the final calculations fairly simple and efficient.

First the division of Ω into elements. In \mathbb{R} we can view Ω as an interval which can be divided into subintervals called elements: $e_k = [z_{k-1}, z_k]$, this means that they are disjoint almost everywhere. Note that it is not required for the elements to have the same length, moreover the union of all the elements equals Ω . This is actually an important property of the elements, this allows us to find the integral over Ω by evaluating the sum of integrals over each element separately.

Because of this property it would be wise to define the basis functions on each element separately:

$$\int_{\Omega} (\phi_p L\phi_q - \phi_p f) d\Omega = \sum_{k=1}^{N-1} \int_{e_k} (\phi_p L\phi_q - \phi_p f) d\Omega. \quad (3.5)$$

Moreover the sum of these integrals will be much easier to evaluate if the basis functions are zero in all but a few elements. These remarks motivate the following properties of the basis functions:

- (1) : ϕ_q is linear in each element,
- (2) : $\phi_q(x_p) = \delta_{pq}$.

These properties uniquely define a set of basis functions. The typical shape of a basis function is graphically presented in Figure 3.1. We leave it to the reader to confirm that these basis functions indeed satisfy the constraints imposed by the weak form.

With this choice of basis function we shall evaluate the system of Galerkin Equations. Because of Equation (3.5) it suffices to evaluate each element e_k separately and add them together afterwards. This motivates matrix and vector notation since we have an equation for every test function ϕ_p and this equation is the sum of integrals over elements e_k . On element $[z_{k-1}, z_k]$ the only functions that have a non-zero contribution are ϕ_{k-1} and ϕ_k . This means that at most 6 of the integrals over an element differ from zero. We shall store these integrals locally in a matrix called the *element-matrix* and a vector called the *element-vector*. The element-matrix is given

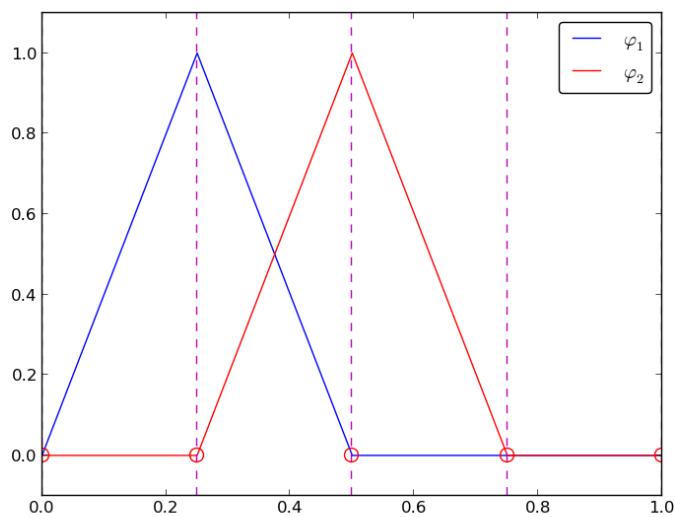


Figure 3.1: An example of two basisfunctions. This image is copied from [CBC n.d.].

by:

$$S^{e_k} = \begin{bmatrix} \int_{e_k} (\phi_{k-1} L \phi_{k-1}) d\Omega & \int_{e_k} (\phi_{k-1} L \phi_k) d\Omega \\ \int_{e_k} (\phi_k L \phi_{k-1}) d\Omega & \int_{e_k} (\phi_k L \phi_k) d\Omega \end{bmatrix}. \quad (3.6)$$

In the same way we can construct the *element-vector*:

$$f^{e_k} = \begin{bmatrix} \int_{e_k} \phi_{k-1} f d\Omega \\ \int_{e_k} \phi_k f d\Omega \end{bmatrix}. \quad (3.7)$$

These elements are relatively small and it is convenient to evaluate these with simple well-known numerical rules such as the trapezoid rule. Once all the element-matrices and element-vectors are computed it is a matter of assembling to obtain the large matrix S and the large vector F to obtain the Galerkin Equations from Equation (3.4) as a matrix-vector product:

$$S\bar{u} = F. \quad (3.8)$$

3.2.1 Assembly of the large matrix and vector

We have seen that all the information for the approximation is stored locally in the element-matrices and element-vectors. From this local form of information we have

to construct the large matrix and vector. This construction is called ‘assembly’. The best way to look at the assembly is with an example, therefore the reader is referred to Appendix B for a comprehensible example. This should make the following, more general approach, easier to understand.

If we want to construct a matrix $S_{pq} = [\int_{\Omega} (\phi_p L \phi_q) d\Omega]$ from the element-matrices then we have to, by Equation (3.5), add the contributions of the element-matrices in such a way that the topology of the problem is not disturbed. The observation that basisfunction ϕ_p only has a contribution on element e_{p-1} and e_p is an important factor. Therefore, we only have to add the entry of an element-matrix to the right entry in the large matrix. In this one dimensional approach: we have to add entry $S_{i,j}^{e_k}$ to $S_{k+(i-1),k+(j-1)}$, perform this for all the entries of every element-matrix and the assembly of the large matrix is complete. The assembly of the large vector is done in an analogous way.

3.3 Moving Mesh Method

In this research we use a Moving Mesh Method to track the interface between the concentrated and dilute phase at $z = z_{\Gamma}$. In general the location of the interface is not situated on a point in the mesh. Even if initially z_{Γ} was located on a mesh point, then after some arbitrary time the interface will have moved and is not necessarily located on a mesh point. This inability to track the interface precisely gives rise to discretisation errors, because numerical values can only be evaluated on mesh points we have to approximate the location of the interface with the nearest mesh point. With a moving mesh we would like to minimize this effect.

The Moving Mesh method ensures that the location of the interface is always precisely on a mesh point. The idea is that we give every point in the mesh a velocity $v_{\text{mesh}}(z, t)$ such that the location of the interface stays on the same mesh point, i.e. $z_{\Gamma}(t_{n+1}) = z_{\Gamma}(t_n) + v_{\Gamma}(z_{\Gamma}(t_n)) \Delta t$. Note the approximation that for small time steps the velocity of the interface v_{Γ} is constant during the timestep. Moreover, the boundary points of the mesh must remain constant, i.e. $z_0(t_{n+1}) = z_0(t_n)$ and $z_{\text{max}}(t_{n+1}) = z_{\text{max}}(t_n)$. The choice for $v_{\text{mesh}}(z)$ is arbitrary, as long as the topology of mesh points remains

unaltered. We have used the following linear extension:

$$v_{\text{mesh}}(z, t) = \begin{cases} v_{\Gamma} \frac{z}{z_{\Gamma}} & \text{for } z \in [0, z_{\Gamma}] \\ v_{\Gamma} \left(1 - \frac{z - z_{\Gamma}}{z_{\text{max}} - z_{\Gamma}}\right) & \text{for } z \in [z_{\Gamma}, z_{\text{max}}] \end{cases} \quad (3.9)$$

Provided that: $-z_{\Gamma} < v_{\Gamma} \Delta t < z_{\text{max}} - z_{\Gamma}$

The above mesh velocity has all the desired properties if it satisfies the condition described in the above equation. For a thorough analysis on this matter, the reader is referred to Appendix C.

The Moving Mesh has an important effect on the concentration profiles. Whereas before the time derivative of the concentration only had a physical meaning, change due to a flux gradient, now there is also a non-physical contribution, change due to moving mesh points. This contribution exists because we introduced a time dependency of the grid points. We will have to take this non-physical effect into account in the diffusion equation and also in our discretisation. Therefore we will look at the total-time derivative of a concentration profile:

$$\frac{dc(z(t), t)}{dt} = \frac{\partial c}{\partial t} + \frac{dz}{dt} \frac{\partial c}{\partial z}. \quad (3.10)$$

Using Equation (2.1) and the fact that $\frac{dz}{dt}$ equals the mesh velocity we can write this as:

$$\frac{dc(z(t), t)}{dt} = -\frac{\partial J}{\partial z} + v_{\text{mesh}}(z(t)) \frac{\partial c}{\partial z}. \quad (3.11)$$

Also, in the discrete sense, if $v_{\text{mesh}}(t_n)$ is known then we can calculate the new mesh:

$$z_m(t_{n+1}) = z_m(t_n) + v_{\text{mesh}}(z_m(t_n)) \Delta t, \quad \text{for } m = 0 \dots N. \quad (3.12)$$

To conclude: a Moving Mesh that tracks the interface introduces a non-physical effect on the change of concentration. For this it is necessary that the interface velocity at each timestep is known so that a proper extension to a mesh velocity can be made. Further, we took a closer look to the diffusion equation by inspecting the total time derivative as can be seen in Equation (3.11) which is to be evaluated on the updated mesh described iteratively by Equation (3.12).

3.4 Galerkin Equations of the Moving-Mesh Diffusion Equation

In this section we will combine the theory from Galerkin's Method, FEM and the Moving Mesh to derive an expression for the concentration profiles after a time step of Δt . In order to do that we first consider the Galerkin Equations of our PDE. For convenience we postulate our diffusion equation again in its full form for each chemical component i :

$$\begin{aligned} \frac{dc_i(z(t), t)}{dt} &= -\frac{\partial J_i}{\partial z} + v_{\text{mesh}}(z(t)) \frac{\partial c_i}{\partial z}, \\ &= -D_i \frac{\partial}{\partial z} \left(\frac{\partial c_i(z(t), t)}{\partial z} + \beta_i c_i(z(t), t) \frac{\partial \psi(z, t)}{\partial z} \right) + v_{\text{mesh}}(z(t)) \frac{\partial c_i}{\partial z}. \end{aligned} \quad (3.13)$$

With $\beta_i = \frac{Z_i F}{RT}$.

From here on we denote $c_i(z(t), t) = c_i$ and $\psi(z, t) = \psi$ to avoid notational clutter. Completely analogous to previous sections we start with approximating $c_i(z(t), t)$ with a finite linear combination of basis functions ϕ_q , multiply this by some test function ϕ_p and integrate over the domain Ω . For the left-hand side we obtain:

$$\frac{dc_i}{dt} \implies \sum_{q=1}^k \frac{dc_{i,q}}{dt} \int_{\Omega} \phi_p \phi_q dz, \quad (3.14)$$

For the right hand side we can apply the same calculations, only we do this for each term separately. But first we note that it is possible to reduce the order of the derivatives corresponding to the flux by using integration by parts. This gives:

$$\begin{aligned} -D_i \frac{\partial J_i}{\partial z} &\implies - \int_{\Omega} D_i \phi_p \frac{\partial J_i}{\partial z} dz, \\ &= -D_i \phi_p J_i \Big|_{\partial\Omega} + \int_{\Omega} D_i \frac{d\phi_p}{dz} J_i dz. \end{aligned} \quad (3.15)$$

It should be clear that the values at the boundary $\partial\Omega$ vanish due to the boundary conditions. Now that we have reduced this expression to the lowest possible order

we rewrite the integral into two distinct terms:

$$\begin{aligned} \int_{\Omega} D_i \frac{d\phi_p}{dz} J_i dz &= \int_{\Omega} D_i \frac{d\phi_p}{dz} \left[\frac{\partial c_i}{\partial z} + \beta_i c_i \frac{\partial \psi}{\partial z} \right] dz, \\ &= \int_{\Omega} D_i \frac{d\phi_p}{dz} \frac{\partial c_i}{\partial z} dz + \int_{\Omega} D_i \beta_i c_i \frac{d\phi_p}{dz} \frac{\partial \psi}{\partial z} dz. \end{aligned} \quad (3.16)$$

Now we are ready to use the FEM approximations for the variables c_i and ψ in Equation (3.16):

$$\int_{\Omega} D_i \frac{d\phi_p}{dz} \frac{\partial c_i}{\partial z} dz = D_i \sum_{q=1}^k c_{i,q} \int_{\Omega} \frac{d\phi_p}{dz} \frac{d\phi_q}{dz} dz, \quad (3.17)$$

$$\int_{\Omega} D_i \beta_i c_i \frac{d\phi_p}{dz} \frac{\partial \psi}{\partial z} dz = D_i \beta_i \sum_{q=1}^k \psi_q \int_{\Omega} c_i \frac{d\phi_p}{dz} \frac{d\phi_q}{dz} dz. \quad (3.18)$$

Note that we did not use the approximation for c_i in Equation (3.18). As we shall see later on, leaving this term explicit with respect to c_i will make it much easier to evaluate the element-matrices.

Finally we consider the discretisation of the mesh velocity term:

$$v_{\text{mesh}}(z(t)) \frac{\partial c}{\partial z} \implies \sum_{q=1}^k c_{i,q} \int_{\Omega} v_{\text{mesh}}(z(t)) \phi_p \frac{d\phi_q}{dz} dz. \quad (3.19)$$

With all of these results above we can finally write Equation (2.1) as a system of Galerkin Equations. For every p the Galerkin Equation is given by:

$$\sum_{q=1}^k \frac{dc_{i,q}}{dt} \int_{\Omega} \phi_p \phi_q dz = \sum_{q=1}^k \left[D_i c_{i,q} \int_{\Omega} \frac{d\phi_p}{dz} \frac{d\phi_q}{dz} dz + D_i \beta_i \psi_q \int_{\Omega} c_i \frac{d\phi_p}{dz} \frac{d\phi_q}{dz} dz + c_{i,q} \int_{\Omega} v_{\text{mesh}} \phi_p \frac{d\phi_q}{dz} dz \right]. \quad (3.20)$$

3.4.1 Galerkin Equations in Matrix Form

In the previous sections we found the weak formulation for the diffusion equation with the moving mesh taken into account, Equation (2.1). The system of Galerkin Equations is given in Equation (3.20). In this section we will construct the element-matrices that allow us to write the system of Galerkin Equations as a matrix vector

product. Before we begin we remind that the basisfunction ϕ_p is only nonzero on elements e_p and e_{p-1} . And that we can evaluate the integrals over each element separately.

We shall write Equation (3.20) as:

$$M \frac{d\bar{c}_i}{dt} = S\bar{c}_i + Q(\bar{c}_i)\bar{\psi}, \quad (3.21)$$

where we define \bar{c}_i and $\bar{\psi}$ as the column vectors with the respective coefficients and the matrices $M, S, Q(\bar{c}_i)$ are constructed by there respective element-matrices:

$$M_{pq}^{e_k} = \int_{e_k} \phi_p \phi_q dz, \quad (3.22)$$

$$S_{pq}^{e_k} = D_i \int_{e_k} \frac{d\phi_p}{dz} \frac{d\phi_q}{dz} dz + \int_{e_k} v_{\text{mesh}} \phi_p \frac{d\phi_q}{dz} dz, \quad (3.23)$$

$$Q_{pq}^{e_k}(\bar{c}_i) = D_i \beta_i \int_{e_k} c_i \frac{d\phi_p}{dz} \frac{d\phi_q}{dz} dz. \quad (3.24)$$

We will use the Newton-Cotes formula to evaluate these integrals. We then get the following element-matrices using the construction as was used with FEM:

$$M^{e_k} = \frac{\|e_k\|}{2} \begin{bmatrix} 1 & 0 \\ 0 & 1 \end{bmatrix}. \quad (3.25)$$

$$S^{e_k} = \frac{D_i}{\|e_k\|} \begin{bmatrix} -1 & 1 \\ 1 & -1 \end{bmatrix} + \frac{1}{2} \begin{bmatrix} -v_{\text{mesh}}(z_k) & v_{\text{mesh}}(z_k) \\ -v_{\text{mesh}}(z_{k+1}) & v_{\text{mesh}}(z_{k+1}) \end{bmatrix}. \quad (3.26)$$

$$Q^{e_k}(\bar{c}_i) = \frac{D_i \beta_i}{2\|e_k\|} \begin{bmatrix} -c_i(z_k) - c_i(z_{k+1}) & +c_i(z_k) + c_i(z_{k+1}) \\ +c_i(z_k) + c_i(z_{k+1}) & -c_i(z_k) - c_i(z_{k+1}) \end{bmatrix}. \quad (3.27)$$

So far we have a discretisation of the moving-mesh diffusion equation for each chemical component separately. We shall couple these in one matrix-vector equation. Furthermore we also add the Poisson Equation (2.3), but before we can do that we have to write it in the following matrix-vector form:

$$R\bar{\psi} = \sum_i T_i \bar{c}_i, \quad (3.28)$$

where we can construct R and T_i in a similar way. This gives:

$$R^{e_k} = \frac{1}{\|e_k\|} \begin{bmatrix} -1 & 1 \\ 1 & -1 \end{bmatrix}, \quad (3.29)$$

$$T_i^{e_k} = -\frac{Z_i F}{2\epsilon_0 \epsilon_r} \begin{bmatrix} 1 & 0 \\ 0 & 1 \end{bmatrix}. \quad (3.30)$$

If we combine all the equations for every chemical component and the Poisson equation in matrix form then we get the following system of equations:

$$\mathcal{M} \frac{d\bar{x}}{dt} = \mathcal{S} \bar{x}, \quad (3.31)$$

$$\begin{bmatrix} M & & & & \\ & M & & & \\ & & M & & \\ & & & M & \\ & & & & \emptyset \end{bmatrix} \frac{d}{dt} \begin{bmatrix} \bar{c}_1 \\ \bar{c}_2 \\ \bar{c}_3 \\ \bar{c}_4 \\ \bar{\psi} \end{bmatrix} = \begin{bmatrix} S_1 & & & & Q_1(\bar{c}_1) \\ & S_2 & & & Q_2(\bar{c}_2) \\ & & S_3 & & Q_3(\bar{c}_3) \\ & & & S_4 & Q_4(\bar{c}_4) \\ T_1 & T_2 & T_3 & T_4 & -R \end{bmatrix} \begin{bmatrix} \bar{c}_1 \\ \bar{c}_2 \\ \bar{c}_3 \\ \bar{c}_4 \\ \bar{\psi} \end{bmatrix} \quad (3.32)$$

3.4.2 Boundary conditions

The result of the previous section, Equation (3.31), does not yet account for the boundary conditions. In this section we will develop a general approach for implementing a Dirichlet type boundary condition.

The implementation is done by altering the rows of the matrices of \mathcal{M} and \mathcal{S} in such a way that at time step $n + 1$ the boundary condition is satisfied. The addition of a vector \bar{f} allows to also implement inhomogeneous conditions. The following defines the used row alterations, for a boundary condition at position k :

$$\begin{cases} \text{row}_k(\mathcal{M}) &= \bar{0} \\ \text{row}_k(\mathcal{S}) &= \bar{0} \text{ and } \mathcal{S}_{kk} = 1 \end{cases}$$

We shall verify that this satisfies a general Dirichlet boundary condition and moreover, we shall evaluate the value of \bar{f} at location k to see how this accounts for inhomogeneous boundary conditions. First we shall look at the Dirichlet type boundary condition, this gives for the k^{th} row:

$$\begin{aligned} \text{row}_k(\mathcal{M}) \frac{d\bar{x}}{dt} &= \text{row}_k(\mathcal{S}) \bar{x} + \bar{f}(k), \\ 0 &= \bar{x}(k) + \bar{f}(k), \\ \bar{x}(k) &= -\bar{f}(k). \end{aligned}$$

Therefore by carefully choosing $\bar{f}(k)$ we can satisfy the boundary conditions. It follows that for the homogeneous case we can choose $\bar{f}(k) = 0$ and for the inhomogeneous case we choose $\bar{f}(k)$ to be equal to minus the desired value at time step $n + 1$.

To conclude, in general it is possible to implement Dirichlet type boundary conditions into Equation (3.31) with a few simple steps. We have to alter the rows of the matrices \mathcal{M}, \mathcal{S} corresponding to the location of the boundary condition. Furthermore the addition of a vector \bar{f} containing zeros except for the elements corresponding to the location of the boundary condition allows us to also implement inhomogeneous conditions. This ensures us that \bar{x} satisfies the boundary conditions at time step $n + 1$.

3.5 Time Step

From the previous section we found that we take the boundary conditions into account if we add the vector \bar{f} from the previous section to Equation (3.31). In this section we will use Euler Backward to solve for one time step. This can be done in the following way:

$$\begin{aligned} \mathcal{M} \frac{d\bar{x}}{dt} &= \mathcal{S}\bar{x} + \bar{f}, \\ \mathcal{M} \left(\frac{\bar{x}_{n+1} - \bar{x}_n}{\Delta t} \right) &= \mathcal{S}_{n+1}\bar{x}_{n+1} + \bar{f}_{n+1}, \\ (\mathcal{M} - \Delta t \mathcal{S}_{n+1}) \bar{x}_{n+1} &= (\mathcal{M}\bar{x}_n + \Delta t \bar{f}_{n+1}), \\ \bar{x}_{n+1} &= (\mathcal{M} - \Delta t \mathcal{S}_{n+1})^{-1} (\mathcal{M}\bar{x}_n + \Delta t \bar{f}_{n+1}). \end{aligned} \tag{3.33}$$

Note that this equation cannot be solved directly. This is due to the fact that \mathcal{S}_{n+1} is dependent on \bar{x}_{n+1} . However, as shall be clear in the next section, this is can be done with Fixed Point Iterations. But for now, we take a moment to appreciate the result.

3.6 Fixed Point Iterations

As mentioned before, we will solve Equation (3.33) for \bar{x}_{n+1} using Fixed Point Iterations. First we observe that Equation (3.33) is indeed of the form $\bar{x}_{n+1} = g(\bar{x}_{n+1})$, where g is some function. Then we can solve it with the following iteration:

$$\bar{x}_{n+1}^{m+1} = g(\bar{x}_{n+1}^m) = (\mathcal{M} - \Delta t \mathcal{S}_{n+1}^m)^{-1} (\mathcal{M}\bar{x}_n + \Delta t \bar{f}_{n+1}). \tag{3.34}$$

Moreover we have to make an initial guess, for this we take $\bar{x}_{n+1}^0 = \bar{x}_n$ the value at the previous time. Because the Δt will be small, the change in \bar{x} will also be small. Therefore justifying this initial guess. These iterations will generate a sequence $\{x_{n+1}^m\}_{m \in \mathbb{N}}$ that will converge towards \bar{x}_{n+1} . Thus solving Equation (3.34) for one time step.

3.7 Broyden Iterations

Given all the boundary conditions, we would be able to solve Equation (3.34) and solve all the concentration profiles and the electric potential at t_{n+1} . However, as discussed in Section 2.5, the boundary conditions on the interface are in general unknown. This section contains the theory necessary to find the interface conditions. First we will develop a modification to Newton's method, with this modification the iterations are less laborious to compute. Later we shall use this new method to approximate the interface boundary conditions of each chemical component as well as for the electric potential. Thus making it possible to make a calculation for the unknowns at t_{n+1} .

3.7.1 Newton's Method and modifications

Newton's Method is concerned with finding the root of a set of n nonlinear equations. Written as:

$$\bar{\sigma}(\bar{\chi}) = \bar{0}. \quad (3.35)$$

Where $\bar{\chi}$ is a column vector of n independent variables and $\bar{\sigma}$ the column vector of functions σ_i . Let $\bar{\chi}_j$ be the j^{th} approximation to the solution of Equation (3.35) and $\bar{\sigma}_j = \bar{\sigma}(\bar{\chi}_j)$. Further, let J_j be the Jacobi matrix evaluated at $\bar{\chi}_j$, defined as $J_{i,k} = [\frac{\partial \sigma_i}{\partial \chi_k}]$. Then the following:

$$\bar{\chi}_{j+1} = \bar{\chi}_j - J_j^{-1} \bar{\sigma}_j, \quad (3.36)$$

defines a sequence $\{\bar{\chi}_j\}_{j \in \mathbb{N}}$ that, given a proper initial guess, converges to $\bar{\chi}$.

An important downside of this method is the difficulty in finding the Jacobi matrix. Especially when the partial derivatives are not well-known and laborious to compute. To relieve this difficulty somewhat, we first introduce the following matrix H_j defined by the approximation for the j^{th} Jacobi matrix: $-J_j^{-1} \simeq H_j$. Instead of approximating J_{j+1} after one iteration, we shall update our previous approximation.

Our choice for the initial guess of H_0 is given by the approximations for each partial derivative. The formula corresponding with the update of H_j is given by:

$$H_{j+1} = H_j - (\bar{p}_j^T H_j \bar{y}_j)^{-1} (H_j \bar{\sigma}_{j+1} \bar{p}_j^T H_j), \quad (3.37)$$

where we defined: $\bar{p}_j = \bar{\chi}_{j+1} - \bar{\chi}_j$, and $\bar{y}_j = \bar{\sigma}_{j+1} - \bar{\sigma}_j$. This formula is taken from [Broyden 1965]. We can substitute this into the standard formula for Newton's Method, Equation (3.35), to obtain:

$$\bar{\chi}_{j+1} = \bar{\chi}_j + \alpha H_j \bar{\sigma}_j. \quad (3.38)$$

We introduced α , a parameter which ensures convergence that will be discussed later in Section 3.7.3. This modification to Newton's Method is called Broyden's Method.

3.7.2 Implementation of Broyden's Method

In the previous section we developed Broyden's Method in order to find the root of a set of equations. In this section we will use this new method to find an approximation for the interface conditions. Therefore we begin with the observation that for given interface conditions the Stefan conditions, Equation (2.8), must hold for each of the four chemical components. Therefore if we define a function that has the value of the discrepancy of the Stefan Condition, then all we have to do is find to root of this function. Moreover it followed from Section 2.5 that we have four 'defining parameters' on the interface, it would be logical to choose these parameters as the variables for the Stefan Condition discrepancy function. A straightforward way to formulate the problem of finding these defining parameters is to find the $\bar{\chi} = ([Cl^-]^{IC}, [Cl^-]^{ID}, v_n, \psi^{ID})$ such that:

$$\bar{\sigma}_i(\bar{\chi}) = \bar{0}. \quad (3.39)$$

Each $\bar{\sigma}_i$ corresponds to the discrepancy of the Stefan condition of chemical component i : $\bar{\sigma}_i = ([i]^{IC} - [i]^{ID}) v_n - (J_i^{IC} - J_i^{ID})$.

3.7.3 Assuring Convergence of Broydens Method

Previously we defined a variable α to assure convergence of Broydens Method. In this section we will explain some details about this parameter.

In each iteration of Newton's Method, the previous value is updated. The magnitude and direction of this update are determined by the term $-J^{-1}\bar{\sigma}_j$. Normally, if the initial guess is within the region of convergence, each successive iteration is closer to the root than the previous one. This is due to the fact that analytic evaluation of the Jacobi matrix ensures that the direction (and magnitude) of this update is perfect. In the case of Broyden iterations however, the Jacobi matrix is approximated. With the updated Jacobi matrix we will update our guess with the term $H_j\bar{\sigma}_j$. It is clear that since H_j is an approximation to the Jacobi matrix that the direction and magnitude of the update contain slight deviations. Thus we have introduced an error, and we will update $\bar{\chi}_j$ to $\tilde{\chi}_{j+1}$, instead of to $\bar{\chi}_{j+1}$. In general, the difference between $\tilde{\chi}_{j+1}$ and $\bar{\chi}_{j+1}$ can be arbitrary. Therefore it is not given that the approximation at t_{n+1} is better than the approximation at time t_n . Even worse, $\tilde{\chi}_{n+1}$ might as well be located outside the region of convergence. This is of course a very serious problem.

Before we provide a solution for this problem, we make the following statement. Let $H_j\bar{\sigma}_j$ be an approximation for $-J^{-1}\bar{\sigma}_j$. Further, let $\bar{\chi}_j$ be the j^{th} approximation to $\bar{\chi}$ and define: $\tilde{\chi}_{j+1} = \chi_j + H_j\bar{\sigma}_j$, the updated value with an error such that it is a worse approximation for $\bar{\chi}$ than $\bar{\chi}_j$. Then there must exist a point $\tilde{\chi}'_{j+1}$, somewhere along the line segment $\mathbb{L} = [\chi_j, \tilde{\chi}_{j+1}]$ that is the best possible approximation for $\bar{\chi}$. This statement can be verified as follows: if not every point in \mathbb{L} is a worse approximation then there should exist at least one point that gives the best possible approximation, call this point $\tilde{\chi}_{j+1}$, moreover there exists some $\alpha \in (0, 1)$ such that $\tilde{\chi}_{j+1} = \chi_j + \alpha H_j\bar{\sigma}_j$. This follows from the *Extreme Value Theorem*. A side note, if every point in \mathbb{L} gives a worse approximation for $\bar{\chi}$, then we choose $\tilde{\chi}'_{j+1} = \bar{\chi}_j$ and we can not find a better approximation with this given H_j within \mathbb{L} . In this case we say $\alpha = 0$. Thus the introduction of the parameter α ensures convergence of the Broyden Iterations. One method for finding the value of α is called *Line Search*. However, we will use a more rudimentary approach. This approach is based on the reasonable assumption that if H_j approximates $-J^{-1}$ well enough, then for small α there should always exist a $\tilde{\chi}_{j+1}$ that is a better approximation for $\bar{\chi}$ than $\bar{\chi}_j$. Thus in a trial-and-error fashion, we check every update for given α and if it does not improve our guess then we divide α by 2 until we find a better approximation.

Chapter 4

Implementation

In this section we will present several aspects of the implementation of the theory. Moreover this section will serve as a comprehensive guide into understanding how the implementation works. First of all we will discuss the choice for the initial condition. Then we will present a graphical overview of the numerical algorithm. Later we will discuss several difficulties that arose during implementation and we will state some ideas for improvement to overcome these difficulties.

4.1 Initial Condition

For the initial condition we have taken the two domains to be completely coexisting phases. Therefore for given κ we are able to determine the concentration profiles for the polyelectrolytes in both domains. Further we take the initial concentration profiles for salt to be constant in both domains, and equal to the respective polyelectrolyte concentration in the concentrated domain. This implies a linear electric potential with no jump across the interface.

4.2 Overview of the script

In Figure 4.1 a schematic overview of the script is presented.

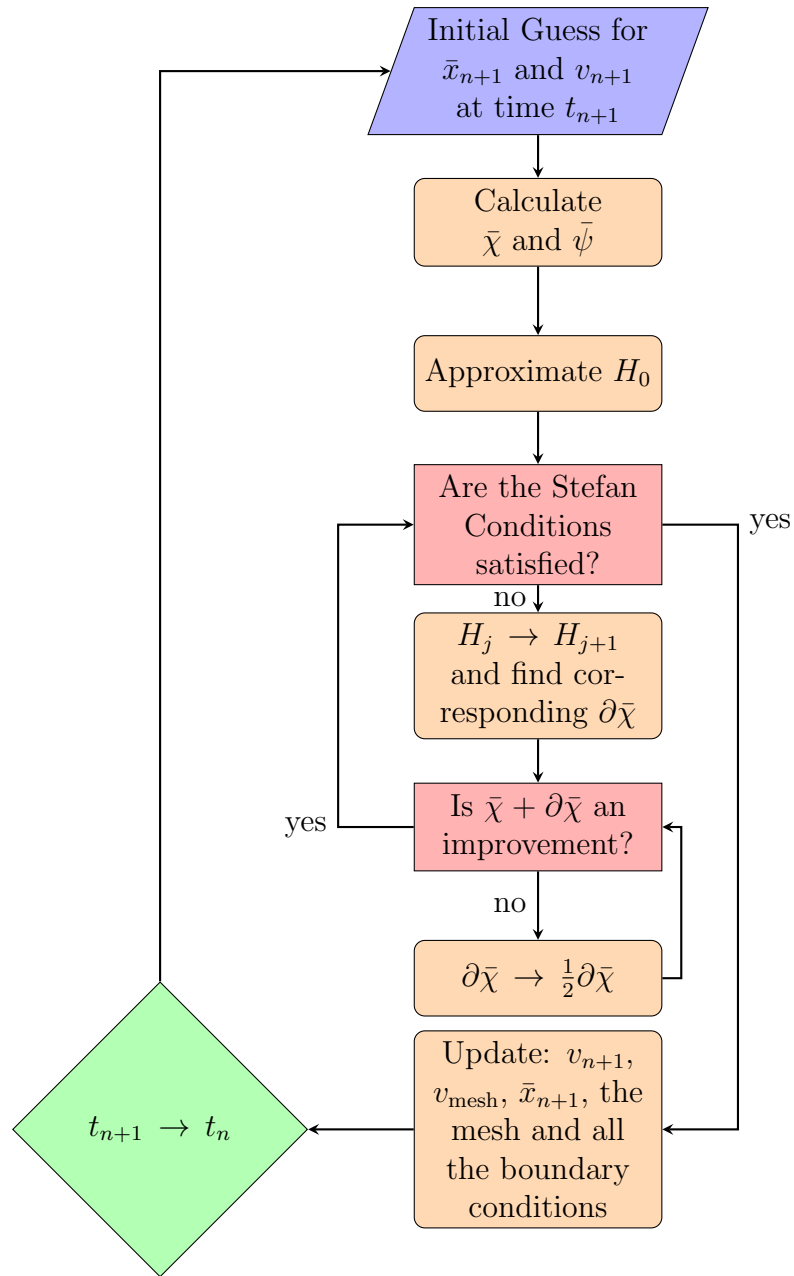


Figure 4.1: A flowchart serving as an overview of the script.

4.3 Difficulties & Discussion

Now we will discuss several difficulties that arose during implementation, and present several ideas to overcome them.

4.3.1 α -Safety-Protocol

This problem concerns to choice of the convergence parameter α . It occurs when, during Broyden iterations, we want to update $\bar{\chi}_j$ when it is actually a very good guess already. As discussed earlier, the code we will try to find an α in a trial-and-error fashion by evaluating the updated guess and if necessary dividing α by 2. Because $\bar{\chi}_j$ is already a good guess the value of α needs to be really small, in the order of 10^{-64} is not uncommon. Because this is done in a trial-and-error fashion, the process of finding such a small α is very time consuming.

One way of reducing time can be by using a better algorithm to find a feasible value for α . However we used a simpler approach. If the update of $\bar{\chi}_j$ was very small, that is to say $|\alpha H_j \bar{\sigma}_j| < 10^{-10}$, then we choose $\alpha = 0$. Clearly the change in $\bar{\chi}_j$ is negligible and thus the given guess is good enough. Therefore we do not need to search for a very small α and we can simply adopt the current guess $\bar{\chi}_j$. We note however, that in general a small α does not necessarily imply a good guess. For example, it might be possible that the build up of approximation errors in $H_j \bar{\sigma}_j$ will result in a erroneous update. In such a case it might be better to make a new (and better) evaluation of H_j and continue the process.

4.3.2 Non-convergence

As discussed earlier, we had great problems with the convergence of our numerical process. This problem cascaded through the whole program, causing difficulties in choosing proper length of time steps, initial guesses and physically logical constants. One culprit is the Fixed-Point iterations Method. This method proved to be the foremost reason for non-convergence. Therefore it would be an improvement to substitute this method with a more rigid numerical technique. Making this process more robust would properly lead to more freedom for experimenting with varying constants and allow a more diverse choice for important coefficients.

4.3.3 Instant Equilibrium Assumption for Small-Ions

One of the great challenges of this method is to track both the evolution of the polyelectrolyte concentration profiles as well as the evolution of the simple salt concentration profiles. This is more difficult than expected because of the widely varying diffusion coefficients. In some cases, the simple salts have a diffusion rate of an order of 10^6 higher than that of the polyelectrolyte. A result of this is that a large number of time steps were needed to simulate the evolution of both of the types of concentration profiles. We think that this allows the build up of errors which leads to erroneous results. A simple suggestion would be to increase the time step, but that leads to convergence problems. However we would like to propose a reasonable assumption which might alleviate this problem.

Since the diffusion coefficient of salt is so much larger than those of the polyelectrolytes, it would be reasonable to assume that the salt concentration profiles assume instant equilibrium at each time step. The steady state solution of Equation (2.1) for given ψ is given by:

$$c^{\text{eq}}(z, t) = c^{\infty} e^{\frac{z_i q}{kT} \psi(z, t)}, \quad (4.1)$$

where c^{∞} is some constant defined by the boundary conditions. Our suggestion is that we replace Equation 3.13 by a correctly discretised expression based on this steady state solution. Possibly this assumption will make it possible to reduce the number of time steps necessary to track the evolution of polyelectrolyte concentration profiles. Thus reducing the calculation time.

Chapter 5

Results

In this section we will explain the main results that led to important conclusions. First we will discuss what properties are not allowed in a tie-line. Secondly we will discuss the two obstacles that arose during simulations. These are: “oscillations in the concentration profiles near the substrate” and “non-responsive interface”.

5.1 Inconsistency in the Tie Lines

During the research, we found that there exist some restrictions on the tie line model for phase separation. Appendix D contains one example of such an inconsistent model. The use of such a model in the implementation will lead to a numerical catastrophe. Thus, during the research, we deduced a constraint for the tie line model. Using the simplification for the binodal curves as discussed in the paper, any tie line that has the following property:

$$[+]^C + [-]^C = [+]^D + [-]^D \neq 0, \quad (5.1)$$

is *inadmissible*. Note however that only the tie line for which this property applies is inadmissible. However since any tie line may be used during phase coexistence, it would be wise to choose a tie line model with only admissible tie lines.

The derivation of this condition starts with the fundamental equations of electro-

neutrality at the interface:

$$\begin{cases} [Na^+]^{IC} = -[Cl^-]^{IC} - ([+]^{IC} + [-]^{IC}), \\ [Na^+]^{ID} = -[Cl^-]^{ID} - ([+]^{ID} + [-]^{ID}). \end{cases} \quad (5.2)$$

We introduce the notation: $\Sigma^I = [+]^I + [-]^I$. Combination of this in the interface equilibrium condition, Equation (2.20), results in:

$$(-[Cl^-]^{IC} - \Sigma^{IC}) [Cl^-]^{IC} = (-[Cl^-]^{ID} - \Sigma^{ID}) [Cl^-]^{ID}.$$

This can be rewritten into:

$$-\Sigma^{IC} [Cl^-]^{IC} + \Sigma^{ID} [Cl^-]^{ID} = ([Cl^-]^{IC})^2 - ([Cl^-]^{ID})^2.$$

Now we assume $\Sigma = \Sigma^{IC} = \Sigma^{ID}$. If $\Sigma = 0$ then Equation (5.2) would immediately simplify. However if $\Sigma \neq 0$, then the previous equation allows for some simplification:

$$\begin{aligned} -\Sigma ([Cl^-]^{IC} - [Cl^-]^{ID}) &= ([Cl^-]^{IC} - [Cl^-]^{ID}) ([Cl^-]^{IC} + [Cl^-]^{ID}), \\ \Sigma &= -([Cl^-]^{IC} + [Cl^-]^{ID}). \end{aligned}$$

And thus, from Equation (5.2) we find:

$$\begin{cases} [Na^+]^{IC} = [Cl^-]^{ID}, \\ [Na^+]^{ID} = [Cl^-]^{IC}, \end{cases} \quad (5.3)$$

Since these $[Na^+]$ and $[Cl^-]$ have opposite signs, the only solution would be the trivial solution:

$$[Na^+]^{IC} = [Na^+]^{ID} = [Cl^-]^{IC} = [Cl^-]^{ID} = 0. \quad (5.4)$$

This is an unlikely result. Therefore we conclude that a tie line with the property: $\Sigma^{IC} = \Sigma^{ID} \neq 0$ is inadmissible.

5.2 Simulations

During the simulations we concluded that the current implementation is unable to correctly simulate the concentration profiles. In this section we will show which difficulties prevented a decent simulation. These difficulties arose near the boundary corresponding to the substrate and on the interface. Moreover we will also show that we can correctly simulate the inflow into the dilute domain

5.2.1 Profiles near the Substrate

In Figure 5.1 we see the concentration profiles of the polyelectrolytes, globally and zoomed in near the interface. In this simulation there exist negative concentrations. We think that the reason for these values is that the initial guess does not account for the electrostatic interactions near the substrate. The numerical iterations will diverge here, thus leading to unfeasible values.

Also in this simulation, one can see that the inflow into the dilute domain is very similar to the expected penetration of a high concentration solution in a diffusion-only medium. This leads us to believe that this model does properly simulate diffusion near the inflow boundary and away from the substrate or on the interface.

5.2.2 Non-Responsive Interface

Other simulations that were performed concerned the behaviour of the polyelectrolytes on the interface. In this simulation we have inflow of polyelectrolytes and we tried to simulate the growth of the PEM. In order to do this we had to make a few adjustments to the model, because otherwise the errors near the substrate would cause the simulation to diverge before there would be any possibility of interface manipulation. Therefore we chose the dilute domain to be relatively short, also we chose a very high inflow of polyelectrolytes. By doing this we were able to significantly alter the conditions on the dilute side of the interface.

In Figure 5.2 we can see how the concentration profiles have evolved with this setup. Because of the high concentration inflow, we would expect the PEM to grow, however the position of the interface remained unchanged. From this we conclude that the model of phase separation is too simplistic to realistically model the behaviour of the interface, as we expect a change in the location of the interface.

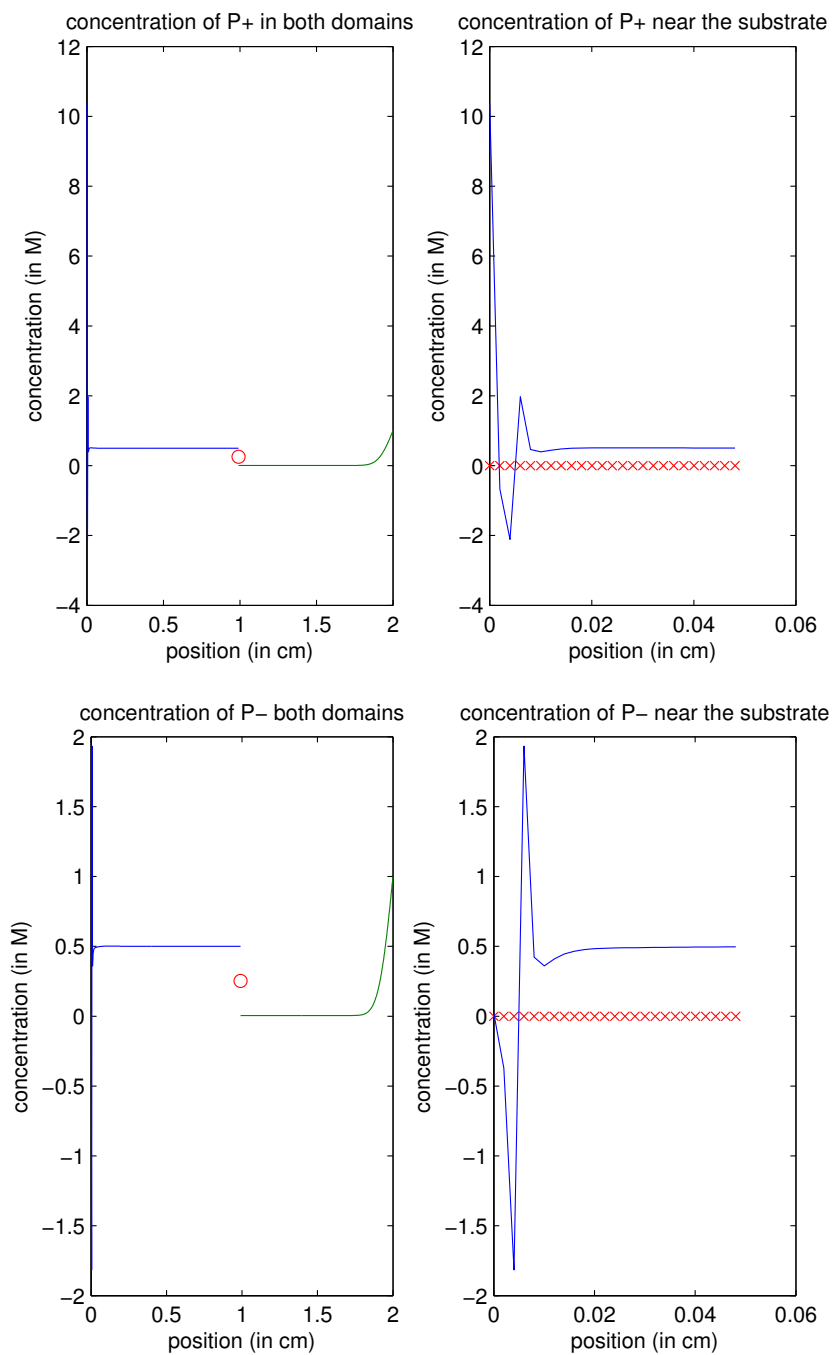


Figure 5.1: Global polyelectrolyte concentration profiles together with a zoom near the substrate. The red dot denotes the position of the interface. The red crosses highlight the zero-concentration line

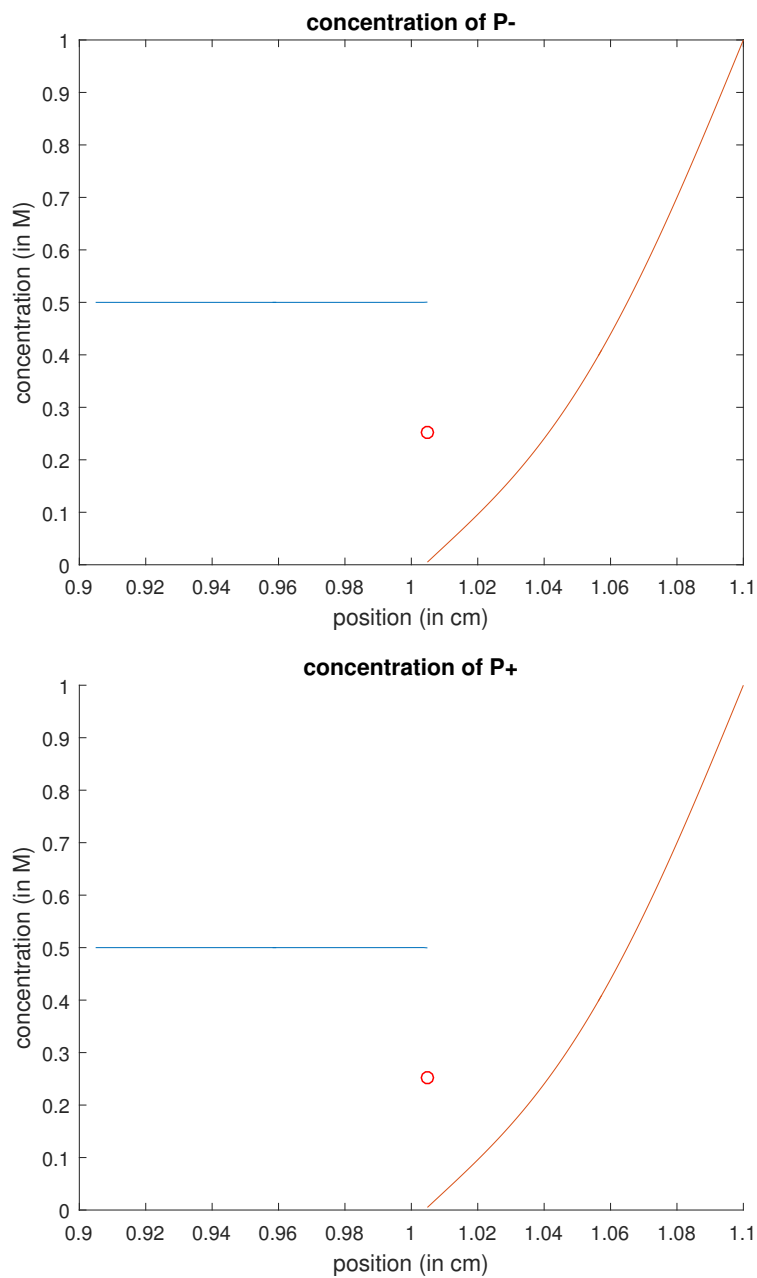


Figure 5.2: Concentrations profiles of the polyelectrolytes with high inflow. In this case $v_n = 3.57 \cdot 10^{-4}$. The red dot denotes the position of the interface.

Chapter 6

Conclusions and Discussion

In this research we were not able to fully describe the evolution of PEM over time. However we believe that this approach to PEM growth is promising. For example we were able to simulate the penetration of high concentrations on the inflow boundary.

Also, we found that not every tie line is admissible, leading to inconsistent models of phase separation if one were to be used. This is a fundamental result which follows from the equilibrium equations on the interface and electro-neutrality.

Another important observation is that the setup for PEM growth, high polyelectrolyte inflow, had no significant effect on the movement of the interface. During the simulations, the Stefan Conditions are properly satisfied, thus leading us to believe that the model on the interface is too simplistic. We recommend that for future research a more elaborate approach for describing the behaviour of chemical components on the interface is investigated.

During simulations we found that the concentration profiles near the substrate contain *negative* values. We will give a suggestion on the origin of this error:

On the substrate boundary we have an in-homogeneous Dirichlet boundary condition for the potential. Physically speaking, the substrate has a fixed, in our case negative, electric potential value. Then it follows from electrostatic interactions that the poly-cations are attracted towards the substrate and the poly-anions are repelled. In theory the poly-cations will reverse the surface charge of the substrate, the poly-anions will then reverse the resulting surface charge of the poly-anions and so on. We expect that this effect should be damped out. However, in our simulations this effect is not damped out and thus in following time steps the oscillations intensify

until concentrations become negative, numerical iterations diverge soon thereafter. Because of this simulation we expect that the initial guess near the substrate is not sufficiently chosen. For future research we recommend that the concentrated domain is not chosen as a completely homogeneous coexisting phase, but that it is such that the electrostatic interactions with the substrate's surface charge are in equilibrium. One example might be as presented in Figure 6.1. The use of the upwind Petrov-Galerkin Method might be a numerical alternative to stabilize the solution and avoid any unrealistic oscillations.

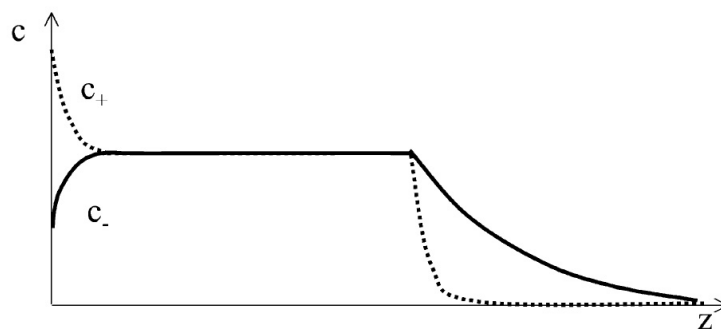


Figure 6.1: One example of an initial guess, this image is copied from [Schönhoff 2003]

Furthermore we recommend that future research will incorporate the instant-equilibrium assumption for the small-ions. Since the different chemical components have greatly varying diffusion coefficient, many time steps are needed to accurately describe the movement of all the chemical components. We think that this reasonable assumption will make to researcher able to better simulate the PEM behaviour.

Appendix A

Derivation of the Stefan Condition

In this section we shall give an elaborate explanation of the origin of the Stefan Condition. This condition is often used in moving boundary value problems, for example the interface between two phases. The Stefan Condition is a reformulation of the conservation of mass principle and therefore, in our research, it must hold for every chemical component independently. It is sufficient to derive this condition for an arbitrary chemical element in a two phase environment and then subject every chemical component to it.

To begin, we define $M(t)$ as the total mass of the chemical element in the entire domain. Since our domain has no sources present, the only way the total mass can change is by the flux across its boundaries. We assumed a no-flux boundary at $z = 0$, Equation (2.4) and therefore it must hold that:

$$\frac{dM(t)}{dt} = -J(z_{max}). \quad (\text{A.1})$$

Now we focus our attention on an expression for $M(t)$. An intuitive way is to integrate the concentration profile across the entire domain. Since we have two distinct phases, we can integrate over each separately. This results in the following:

$$M(t) = \int_0^{z_{\Gamma}(t)} c^C(z, t) dz + \int_{z_{\Gamma}(t)}^{z_{max}} c^D(z, t) dz. \quad (\text{A.2})$$

We can also try to find an expression for the derivative of $M(t)$. Because of the

linearity of the derivative we can say:

$$\frac{dM(t)}{dt} = \frac{d}{dt} \left(\int_0^{z_\Gamma(t)} c^C(z, t) dz \right) + \frac{d}{dt} \left(\int_{z_\Gamma(t)}^{z_{max}} c^D(z, t) dz \right). \quad (\text{A.3})$$

We can not evaluate these terms directly because the interval over which we integrate is dependent on time. However, if we assume that there exists some antiderivative $F(z, t)$ of $c^C(z, t)$ with respect to z , we get the following expression:

$$\frac{d}{dt} \left(\int_0^{z_\Gamma(t)} c^C(z, t) dz \right) = \frac{d}{dt} \left(F(z_\Gamma(t), t) - F(0, t) \right), \quad (\text{A.4})$$

note that the right hand side can be solved with use of the chain rule:

$$\frac{d}{dt} \left(F(z_\Gamma(t), t) - F(0, t) \right) = \frac{\partial F}{\partial z} \Big|_{z=z_\Gamma} \frac{dz_\Gamma}{dt} + \frac{\partial F}{\partial t} \Big|_{z=z_\Gamma} - \frac{\partial F}{\partial t} \Big|_{z=0}. \quad (\text{A.5})$$

The physical meaning of $\frac{dz_\Gamma}{dt}$ is the speed at which the location of the interface moves. We call this speed the *normal velocity* v_n , where the normal vector of the interface is pointing outward of $\Omega_C(t)$. Now we try to eliminate the function $F(z, t)$ from the right-hand side of Equation (A.5):

$$\frac{\partial F}{\partial z} \Big|_{z=z_\Gamma} \frac{dz_\Gamma}{dt} + \frac{\partial F}{\partial t} \Big|_{z=z_\Gamma} - \frac{\partial F}{\partial t} \Big|_{z=0} = c^C(z_\Gamma(t), t) v_n + \int_0^{z_\Gamma(t)} \frac{\partial c^C}{\partial t}(z, t) dz, \quad (\text{A.6})$$

according to the Fundamental Theorem of Calculus. From the diffusion equation it follows that:

$$\frac{\partial c^C}{\partial t}(z, t) = -\frac{\partial J^C}{\partial z}(z, t), \quad (\text{A.7})$$

and therefore:

$$\int_0^{z_\Gamma(t)} \frac{\partial c^C}{\partial t}(z, t) dz = - \int_0^{z_\Gamma(t)} \frac{\partial J^C}{\partial z}(z, t) dz = -J^C(z_\Gamma(t), t) + J^C(0, t) = -J^C(z_\Gamma(t), t). \quad (\text{A.8})$$

Note that $J^C(0, t) = 0$ because of the no-flux boundary condition we imposed at $z = 0$. If we combine Equations (A.4) to (A.8), then we end up with:

$$\frac{d}{dt} \left(\int_0^{z_\Gamma(t)} c^C(z, t) dz \right) = c^C(z_\Gamma(t), t) v_n - J^C(z_\Gamma(t), t). \quad (\text{A.9})$$

We can repeat these steps in a similar fashion for the integral over the dilute phase in Equation (A.3). Note the important difference $J^D(z_{max}, t) \neq 0$ because we use a different boundary condition at $z = z_{max}$. We can find the expression:

$$\frac{d}{dt} \left(\int_{z_\Gamma(t)}^{z_{max}} c^D(z, t) dz \right) = -c^D(z_\Gamma(t), t)v_n + J^D(z_\Gamma(t), t) - J^D(z_{max}, t). \quad (\text{A.10})$$

The final step is to combine Equations (A.1), (A.3), (A.9) and (A.10) to obtain:

$$c^C(z_\Gamma(t), t)v_n - J^C(z_\Gamma(t), t) = c^D(z_\Gamma(t), t)v_n - J^D(z_\Gamma(t), t), \quad (\text{A.11})$$

or in more convenient notation:

$$c^{IC}(t)v_n(t) + J^{IC}(t) = c^{ID}(t)v_n(t) + J^{ID}(t). \quad (\text{A.12})$$

We have arrived at the Stefan Condition in its final form. Each side of Equation (A.12) has unit $[mol\ m^{-2}s^{-1}]$, the unit of flux. This is logical if we take another look at Equation (A.12). It relates the difference in fluxes across the interface, which is equivalent to accumulation of mass, to the growing of the concentrated phase, which is equivalent to the moving interface. This fact is more intuitive if we write the Stefan Condition as: $(c^{IC} - c^{ID})(t)v_n(t) = (J^{IC} - J^{ID})(t)$. Here we can also see *why* an interface in a two phase setting tends to change. Because the two phases have different diffusion coefficients there can be a difference of flux across the interface. This mass has to go somewhere, or has to come from somewhere. The only option to account for this is movement of the interface. Another important aspect is that this equation gives information about the movement of the interface, since we can find v_n if we know all the concentrations and fluxes on either side of the interface. This is extremely important for simulations of the growth of PEMs.

Appendix B

Assembly of the Large Discretisation Matrix

We shall give the reader a simple and comprehensible example for the assembly of a large matrix from several element matrices. For simplicity we consider 3 elements of the same size and we say that the element matrices are given by:

$$S^{e_k} = \begin{bmatrix} 1 & 1 \\ 1 & 1 \end{bmatrix}, \text{ for every } k \in (1, 2, 3).$$

Next, we start with an empty large matrix. Iteratively we shall add the contributions of every element-matrix. This yields the following calculations.

$$S^{e_1} = \begin{bmatrix} 1 & 1 \\ 1 & 1 \end{bmatrix} \implies S = \begin{bmatrix} \boxed{1 & 1} & 0 & 0 \\ 1 & 1 & 0 & 0 \\ 0 & 0 & 0 & 0 \\ 0 & 0 & 0 & 0 \end{bmatrix}$$

$$S^{e_2} = \begin{bmatrix} 1 & 1 \\ 1 & 1 \end{bmatrix} \implies S = \begin{bmatrix} 1 & 1 & 0 & 0 \\ 1 & \boxed{2 & 1} & 0 \\ 0 & 1 & 1 & 0 \\ 0 & 0 & 0 & 0 \end{bmatrix}$$

$$S^{e_3} = \begin{bmatrix} 1 & 1 \\ 1 & 1 \end{bmatrix} \implies S = \begin{bmatrix} 1 & 1 & 0 & 0 \\ 1 & 2 & 1 & 0 \\ 0 & 1 & \boxed{2 & 1} \\ 0 & 0 & 1 & 1 \end{bmatrix}$$

The process terminates after the last element. We have successfully assembled the large matrix S . The assembly of a large vector is very similar.

Appendix C

Derivation of the Mesh-Velocity Constraint

In this section we are going to derive the conditions under which the linear mesh velocity, chosen in Equation (3.9), satisfies two conditions. First condition, we want our mesh to remain within the domain, therefore the boundary of our domain should have zero velocity. In our case this leads to: $v_{\text{mesh}}(0, t) = v_{\text{mesh}}(z_{\text{max}}, t) = 0$. Secondly, the topology of our mesh must not change. Equivalently in discrete terms, at time n for every point z_k^n after time step Δt it must hold that $z_k^{n+1} < z_{k+1}^{n+1}$.

We remind that the linear mesh velocity is given by:

$$v_{\text{mesh}}(z, t) = \begin{cases} v_{\Gamma} \frac{z}{z_{\Gamma}} & \text{for } z \in [0, z_{\Gamma}] \\ v_{\Gamma} \left(1 - \frac{z - z_{\Gamma}}{z_{\text{max}} - z_{\Gamma}}\right) & \text{for } z \in [z_{\Gamma}, z_{\text{max}}] \end{cases}$$

It should be clear that for $z = 0$ and $z = z_{\text{max}}$ the velocity reduces to zero. Thus satisfying the first property. Now we assume that at time n the mesh has a well defined topology $z_k^n < z_{k+1}^n$. Then after some time step we have $z_k^{n+1} = z_k^n + \Delta t v_{\text{mesh}}(z_k^n)$, analogous for z_{k+1}^{n+1} . Then, at time $n + 1$ it should follow that:

$$z_{k+1}^{n+1} - z_k^{n+1} > 0,$$
$$(z_{k+1}^n - z_k^n) + \Delta t (v_{\text{mesh}}(z_{k+1}^n) - v_{\text{mesh}}(z_k^n)) > 0.$$

Now we consider $z_k^n \in [0, z_\Gamma^n]$, then:

$$(z_{k+1}^n - z_k^n) + \Delta t v_\Gamma \left(\frac{z_{k+1}^n - z_k^n}{z_\Gamma} \right) > 0$$

$$(z_{k+1}^n - z_k^n) \left[1 + \frac{\Delta t v_\Gamma}{z_\Gamma} \right] > 0.$$

Since we assumed that $(z_{k+1}^n - z_k^n) > 0$ it must hold that: $\Delta t v_\Gamma > -z_\Gamma$.
Now consider $z_k^n \in [z_\Gamma^n, z_{\max}^n]$:

$$(z_{k+1}^n - z_k^n) + \Delta t v_\Gamma \left(\frac{z_k^n - z_{k+1}^n}{z_{\max}^n - z_\Gamma^n} \right) > 0,$$

$$(z_{k+1}^n - z_k^n) \left[1 - \frac{\Delta t v_\Gamma}{z_{\max}^n - z_\Gamma^n} \right] > 0$$

Now we can say that it must hold that: $\Delta t v_\Gamma < z_{\max}^n - z_\Gamma^n$. Because we have chosen an arbitrary mesh point k , these conditions should ensure that the topology remains unaffected after a time step.

Combining these conditions we find that the linear mesh velocity has the desired properties if it satisfies the condition:

$$-z_\Gamma < \Delta t v_\Gamma < z_{\max} - z_\Gamma.$$

Appendix D

Example of Inconsistent Tie-Line Model

During the research we found that not every model for the coexisting phases is feasible. In this appendix, we will provide an example of an inconsistent model. This model is of importance because it was the model we initially used, until we found that it was inconsistent.

We choose for the tie lines the set of parallel lines: $[-] = A - [+]$. Furthermore we use the same approximation for the binodal curves:

$$[-]^D = C^D + [+]^D, \quad (\text{D.1})$$

$$[-]^C = C^C + [+]^C. \quad (\text{D.2})$$

Where $C^C < C^D < 0$ Then we obtain the following for phase-separation at the interface:

$$\left\{ \begin{array}{l} [-]^D = \frac{1}{2}(A + C^D) \\ [+]^D = \frac{1}{2}(A - C^D) \\ [-]^C = \frac{1}{2}(A + C^C) \\ [+]^C = \frac{1}{2}(A - C^C) \end{array} \right. \quad (\text{D.3})$$

If we combine this with the equations for electroneutrality:

$$[+]^C + [Na^+]^C = -([-]^C + [Cl^-]^C), \quad (\text{D.4})$$

$$[+]^D + [Na^+]^D = -([-]^D + [Cl^-]^D), \quad (\text{D.5})$$

then we obtain:

$$[Na^+]^C = -(A + [Cl^-]^C), \quad (D.6)$$

$$[Na^+]^D = -(A + [Cl^-]^D). \quad (D.7)$$

From the equilibrium condition on the interface we can easily find:

$$[Na^+]^C [Cl^-]^C = [Na^+]^D [Cl^-]^D, \quad (D.8)$$

$$-(A + [Cl^-]^C) [Cl^-]^C = -(A + [Cl^-]^D) [Cl^-]^D, \quad (D.9)$$

$$\implies A = -([Cl^-]^D + [Cl^-]^C). \quad (D.10)$$

If we combine this expression with Equations (D.6) and (D.7) then we find:

$$[Na^+]^C = [Cl^-]^D, \text{ and } [Na^+]^D = [Cl^-]^C. \quad (D.11)$$

Since the components of the disassociated salt have an opposite sign, the only solution to these equations is the trivial solution: $[Na^+]^C = [Cl^-]^D = [Na^+]^D = [Cl^-]^C = 0$. This is undesirable, because then the only admissible tie line would be $A = 0$ and the model would not hold for every initial unstable mixture. To conclude, the choice of tie lines and binodal curves leaves us with inconsistencies in the model.

Bibliography

- Broyden, C. G. (1965). “A Class of Methods for Solving Nonlinear Simultaneous Equations”. In: *Math. Comp.* 19, pp. 557–596.
- G. Decher, J.D. Hong and J. Schmitt (1992). “Buildup of ultrathin multilayer films by a self-assembly process: III. Consecutively alternating adsorption of anionic and cationic polyelectrolytes on charged surfaces”. In: *Thin Solid Films* 210/211, pp. 831–835.
- Schönhoff, M. (2003). “Self-assembled polyelectrolyte multilayers”. In: *Current Opinion in Colloid and Interface Science* 8, pp. 86–95.
- Tang, K. and N.A.M. Besseling (2015). “Formation of polyelectrolyte multilayers: ionic strengths and growth regimes”. In: *Royal Society of Chemistry*.
- CBC. *Finite element basis functions*. URL: http://hplgit.github.io/INF5620/doc/pub/sphinx-fem/_main_fem003.html.